# Imaging Modalities for Pheochromocytoma and Paraganglioma

7

David Taïeb, Aoife Kilcoyne, Ingo Janssen, Katherine I. Wolf, Michael Austin Blake, and Karel Pacak

## Tumor Origin

Pheochromocytoma (PHEO) and sympathetic-associated paragangliomas (symp-PGL) develop from cells of the adrenal medulla or extra-adrenal chromaffin cells, respectively. Embryogenesis of chromaffin cells has received considerable attention over the last century. Evidence for the origin of adrenal medulla and sympathetic neurons was pursued by a number of research groups, but it was largely the work of Le Douarin and colleagues using quail/chick chimeras that led to the resolution of their neural crest (NC) origin [1]. Later, immunohistochemical studies, in situ hybridization, transgenic animal studies, and single cell electroporation methods using fluorescent NC progenitors, significantly added to the knowledge of the required mechanisms for correct specification, migration, and differentiation of the sympathoadrenal lineage [2]. Chromaffin cells and sympathetic neurons derive from a common sympathoadrenal (SA) progenitor cell. SA progenitor cells aggregate at the dorsal aorta, where they acquire a catecholaminergic neural date. Subsequently, the cells migrate ventrally to invade the fetal adrenal cortex and form the adrenal medulla as well as dorsolaterally to form sympathetic ganglia. Most extra-adrenal chromaffin cells regress via apoptosis. The organ of Zuckerkandl (OZ) constitutes the largest chromaffin paraganglia in the embryo and regresses after birth via autophagy [3]. Adrenal medulla and persistent extra-adrenal chromaffin cells located in the retroperitoneum and posterior mediastinum represent the chromaffin paraganglia system in adults. These embryological bases explain why PHEO and symp-PGL can be widely distributed throughout the body.

## Spectrum of Hereditary Syndromes

Research in molecular genetics has resulted in the identification of 18 susceptibility genes for tumors of the entire paraganglia system. Most PHEOs occur sporadically (>90%) whereas the

D. Taïeb, M.D., Ph.D. (✉)
Biophysics and Nuclear Medicine, European Center for Research in Medical Imaging, La Timone University Hospital, Aix-Marseille University, 264, rue Saint-Pierre, Marseille 13385, France
e-mail: david.taieb@ap-hm.fr

A. Kilcoyne, M.B.B.Ch.
M.A. Blake, M.B.B.Ch.
Division of Abdominal Imaging and Intervention, Department of Radiology, Massachusetts General Hospital, Harvard Medical School, Boston, MA, USA

I. Janssen, M.D. • K.I. Wolf, B.Sc. • K. Pacak, M.D., Ph.D., D.Sc.
Section on Medical Neuroendocrinology, National Institutes of Health Clinical Center, Eunice Kennedy Shriver National Institute of Child Health and Human Development, Bethesda, MD, USA


E. Kebebew (ed.), *Management of Adrenal Masses in Children and Adults*,
DOI 10.1007/978-3-319-44136-8_7

majority of symp-PGLs are associated with germline driver mutations. Depending on their locations, the most commonly found gene mutations are as follows: (1) unilateral PHEO: succinate dehydrogenase complex subunit B (*SDHB*), von Hippel–Lindau tumor suppressor (*VHL*); (2) bilateral PHEO: *SDHB*, Ret Proto-Oncogene (*RET*), VHL, neurofibromin 1 (*NF1*), MYC associated factor X (*MAX*), transmembrane protein 127 (*TMEM127*); (3) symp-PGLs with or without PHEO: *SDHB*, succinate dehydrogenase complex subunit D (*SDHD*), *VHL*, hypoxia-inducible factor 2-alpha, also called EPAS1 (*HIF2A*). Other genes account for a small minority of cases. Tumor sequencing has also led to the identification of somatic events in a large number of PHEOs and PGLs.

## Clinical Presentation

PHEO/PGLs are rare tumors (annual incidence of 0.1–0.6 per 100,000 population). They account for about 4% of adrenal incidentalomas with a higher prevalence in autopsy series. PHEOs and symp-PGLs usually cause symptoms of catecholamine oversecretion (e.g., sustained or paroxysmal elevations in blood pressure, headache, episodic profuse sweating, palpitations, pallor, and apprehension or anxiety).

## Anatomic Imaging

### Computed Tomography (CT)

#### Patient Preparation and Imaging Protocol

At our institution, patients are asked to fast for 2 h [4] prior to the study. To diagnose PHEO, we use a number of CT protocols. The "adrenal nodule protocol" consists of three series—noncontrast, contrast enhanced (at 60 s), and delayed images (at 15 min) of the abdomen. The attenuation of the adrenal nodule is measured on the three series and washout characteristics calculated [4]. In cases where the location of a PHEO is unclear but is clinically or biochemically suspected, a noncontrast CT is ordered. If later deemed necessary, a contrast-enhanced (at 60 s) CT is obtained of the chest, abdomen, and pelvis. Depending on body weight, (80 cc if <180 pounds, 100 cc if <280 pounds, 120 cc if >280 pounds), Isovue 370 is administered. Previously, there have been concerns regarding the administration of iodinated contrast to patients with PHEO. However, we now normally administer contrast. A retrospective review of patients who received nonionic contrast demonstrated the safety of intravenous contrast, even in patients who had not received alpha or beta blockade [5]. A small, prospective study of patients receiving low-osmolar contrast media also demonstrated safety [6]. An occasionally employed, alternative practice is to discontinue the protocol after the noncontrast scan if an adrenal mass or a mass along the sympathetic chain is discovered in a patient suspected of having a PHEO. If considered necessary for diagnosis or surgical planning, we follow with iodinated contrast or an MRI scan, the latter of which would avoid the use of iodinated contrast entirely.

Previously, our studies were performed at 120 kV. We now perform weight-based protocols and in patients less than 200 pounds, we use a lower tube voltage of 100 kV with a usual mA of 300.

#### Normal Appearances and Abnormalities

The adrenal glands are a pair of retroperitoneal, thin, inverted, V or Y shaped organs with flat or concave margins [7]. The vertical length can range from 2 to 4 cm. Both limbs measure approximately 4 mm in cross-section [8].

On noncontrast CT, a PHEO can demonstrate a variety of appearances. They can be low density or of soft tissue attenuation. Two-thirds of PHEO are solid, while the remainder are complex or have undergone cystic change [9]. Reliably differentiating an adenoma from a PHEO can be problematic. Typically, the CT attenuation of PHEO is of soft tissue attenuation and thus, greater than 10 Hounsfield units (HU]. However, in the rare circumstance where a PHEO contains fat, attenuation values can be similar to adenomas, measuring less than 10 HU [10]. PHEO can

be of high attenuation due to the presence of hemorrhage [11]. Although infrequent, calcifications may be present in approximately 10% of cases [12]. PHEO typically demonstrate avid enhancement [13] and any adrenal lesion that enhances greater than 130 HU on multidetector CT cannot be assumed to be an adenoma [14]. In addition, enhancement can be heterogeneous or there may be no enhancement due to cystic or degenerated regions within the lesion. In terms of washout pattern, PHEO can demonstrate varying and nonuniform washout patterns, leading to the inability to reliably differentiate PHEO from adenomas and metastasis to the adrenal gland [10, 15, 16]. A substantial minority of PHEO (33%), especially when hypervascular have washout levels similar to those of adenomas [17].

### Diagnostic Accuracy

To detect PHEO in the adrenal gland, the sensitivity of CT ranges from 76 to 100% [18–21]. Specificity is much lower in distinguishing PHEO, adrenal adenomas, and myelolipomas with figures as low as 50% [18, 20, 21]. Overall sensitivity of CT for the detection of extra-adrenal PHEO as well as recurrent, residual, or metastatic tumors can be as low as 57% [20, 22–24]. Specificity is also low with reported values of 50% [25].

## Magnetic Resonance Imaging (MRI)

### Patient Preparation and Imaging Protocol

At the time of referral, the clinician is responsible for documenting that the patient does not have any contraindications to undergoing MRI. The patient is also asked to verify this on the day of the study.

In patients with suspected PHEO, our MR imaging protocol includes a coronal, breath-hold T2 HASTE; axial, gradient-recalled echo T1 chemical-shift imaging with in- and-out-of-phase breath-hold images; axial fast spin-echo T2-weighted fat-saturated or long TE inversion recovery breath-hold images, as well as axial precontrast and dynamic-enhanced gradient-recalled-echo 3D volumetric interpolated breath-hold examination images. For an abdominal MRI, anatomic coverage should extend from the diaphragm to the aortic bifurcation. In order to also detect extra-adrenal PGLs along the lower sympathetic chain, a pelvic MRI can be added if complete coverage is desired.

As MRI does not confer any ionizing radiation, there is no radiation dose to the patient. This is particularly advantageous in young patients or those who need to undergo repeat imaging.

### Normal Appearances and Abnormalities

The normal adrenal gland demonstrates low to intermediate signal on T1- and T2-weighted imaging [26]. The classic imaging appearance of PHEO is "light-bulb" bright on T2-weighted imaging. In reality, the prevalence of this appearance is low with reported ranges between 1 and 65% of PHEO [27–29] with lowest figures in studies with current technology MRIs. Thirty percent of PHEO demonstrate moderate or low T2-weighted signal intensity [13, 30]. A PHEO is usually hypointense on T1-weighted imaging [13], although the presence of fat or hemorrhaging could lead to high signal intensity on T1. However, PHEO do not usually contain fat and thus, maintain their signal on opposed-phase gradient-echo images [31]. On rare occasions, they can contain microscopic fat leading to signal loss on chemical shift [13]. PHEO typically demonstrate avid contrast enhancement following the administration of intravenous gadolinium-based contrast material [28, 32], similar to enhancement on CT (Figs. 7.1, 7.2, and 7.3). Diffusion-weighted MRI may provide useful additional information for the diagnosis of PHEO. PHEOs have been demonstrated to have relatively higher Apparent Diffusion Coefficient (ADC) values than adrenocortical adenomas and malignancies [33]. MRI spectroscopy is an emerging technique that has shown promise in small cohort studies [34]. A unique spectral signature of PHEO not seen in adenomas was demonstrated using a 2D PACE single-voxel MR spectroscopy sequence [34]. Further evaluation in a larger series will be necessary for validation of this technique.

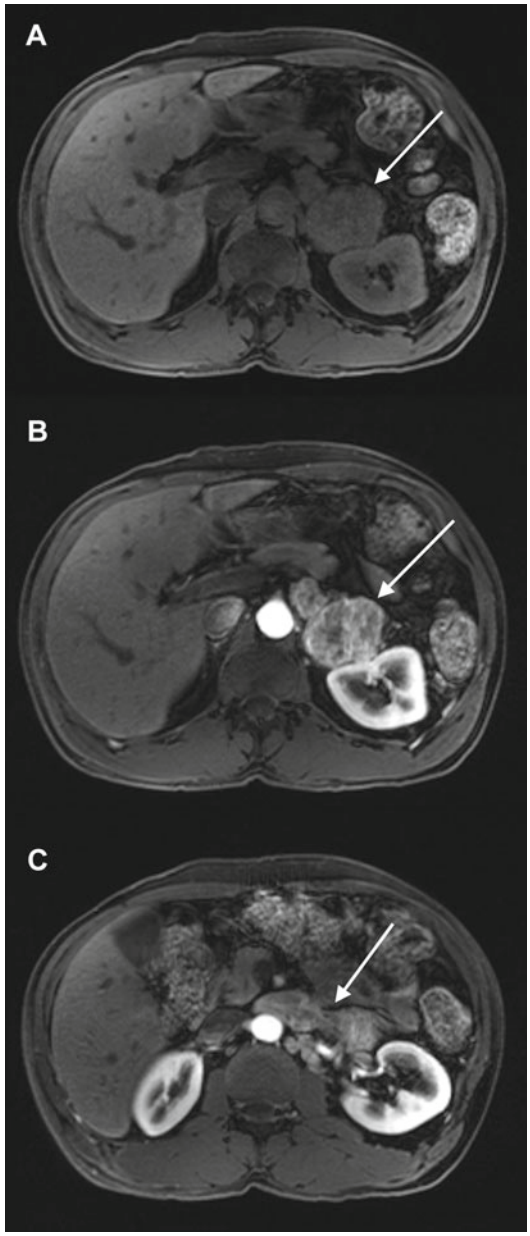


**Fig. 7.1** Fifty-two-year-old man with hypertension. Precontrast, axial T1-weighted image with fat saturation (**a**), demonstrates a large left adrenal mass (*arrow*). On the postcontrast axial T1-weighted image with fat saturation (**b**), there is heterogeneous enhancement (*arrow*). (**c**) (postcontrast axial T1 weighted image with fat saturation) demonstrates invasion of the left renal vein (*arrow*). This was a pathologically confirmed pheochromocytoma

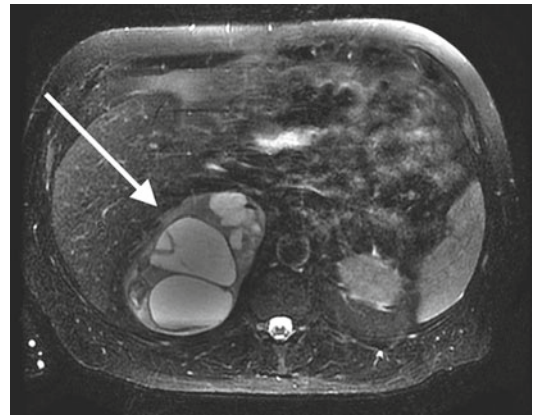

**Fig. 7.2** Seventy-year-old man with incidentally discovered right adrenal mass. Axial, fast spin echo, fat saturated sequence demonstrating an enlarged, heterogeneous right adrenal mass (*arrow*) with hemorrhagic cystic areas within and internal septations. This was confirmed on resection to demonstrate a pheochromocytoma

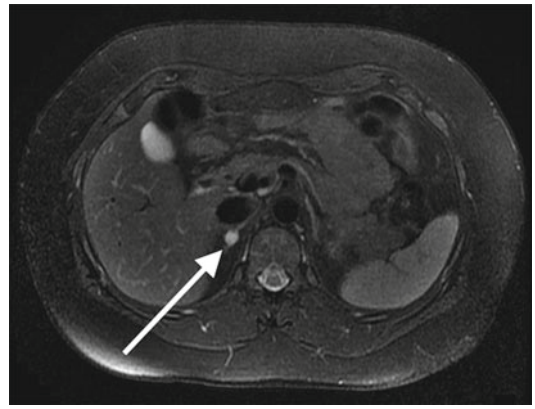

**Fig. 7.3** Twenty-six-year-old woman with von Hippel–Lindau syndrome. Axial T2-weighted image demonstrates a small, T2 bright mass (*arrow*) within the right adrenal gland. This was a pathologically proven pheochromocytoma. This patient had previous resection of the left adrenal gland, which was also a pathologically confirmed pheochromocytoma

## Diagnostic Accuracy

For detecting PHEO in the adrenal gland, the sensitivity of MRI ranges between 91 and 100 % with a specificity of approximately 50–97 % [18, 19, 23, 28, 35]. For the detection of adrenal and extra-adrenal PGLs, the sensitivity is 93 % with a specificity ranging from 50 to 100 % [25, 36]. MRI has been reported as superior to CT for the detection of extra-adrenal tumors [21, 37, 38].

## Malignant PHEO

On imaging, it is difficult to diagnose malignant PHEO in the absence of metastatic disease [12]. The presence of vascular or capsular invasion is

not a pathognomic feature of malignancy, although it is identified more commonly in malignant, rather than benign PHEO [39]. Diffusion-weighted MR imaging can be advantageous in depicting lymph node and liver metastases and may have a higher rate of detecting metastatic lesions compared with Metaiodobenzylguanidine scintigraphy or FDG-PET [40].

## Radionuclide Imaging and Metabotypes

The major advantage of nuclear imaging is in providing a high visual contrast between tumor and healthy tissue, which enables the detection of tumors that could potentially be missed by conventional imaging. Beyond its localization value, this imaging modality provides unique opportunities for enhanced characterization of these tumors at the molecular level (e.g., catecholamine synthesis, transporter expression, somatostatin receptor expression, glucose metabolism), mirroring *ex vivo* histologic classification, but on a whole-body, in vivo, scale [41]. This opportunity is currently possible with a number of excellent radiopharmaceuticals, which target different functional and molecular pathways that often reflect the diverse genetic landscape of PHEO/PGL.

### $^{123}$I-Metaiodobenzylguanidine (MIBG) and Catecholaminergic Phenotype

#### Cellular Uptake and Interference

MIBG is an iodinated analog of guanidine, which is structurally similar to norepinephrine. It is taken up by cells via the norepinephrine transporter and stored within the neurosecretory granules via vesicular monoamine transporters 1 and 2.

Many drugs modify the uptake and storage of MIBG such as opioids, tricyclic antidepressants, sympathomimetics, antipsychotics, and some antihypertensive agents such as Labetalol.

#### Patient Preparation, Imaging Protocol, and Dosimetry

Thyroid blockade is started a day before tracer injection and continued for 2 days after a $^{123}$I-MIBG scan and 5 days for a $^{131}$I-MIBG scan. Discontinuation of drugs interfering with MIBG uptake and retention is required. All medications must be withheld for 1–3 days prior to imaging, with the exception of labetalol and depot forms of antipsychotics, for which the suggested withdrawal period is 1 month.

$^{123}$I-MIBG scintigraphy is preferable to $^{131}$I-MIBG scintigraphy because it provides higher quality images and lower radiation exposure. $^{123}$I -MIBG scans are usually obtained 24 h after tracer injection (200–400 MBq) and consist of planar static images and in adults, SPECT/CT over the anatomical regions showing pathological tracer uptake.

The effective dose for $^{123}$I-MIBG is 0.013 mSv/MBq. The radiation dose is higher when CT is used in SPECT/CT protocols.

#### Normal Distribution and Abnormal Patterns

Normal uptake of $^{123}$I-MIBG can be observed in the myocardium, salivary glands, thyroid gland (if no adequate thyroid blockade is performed), liver, lungs, adrenal glands, and bowel. The large intestine may also be visible. Brown adipose tissue uptake should be considered within the normal distribution of MIBG, although this may be more common in children than adults. $^{123}$I-MIBG uptake in the adrenal glands is considered normal if mild (less or equal to liver uptake), symmetric, and when the glands are not enlarged on CT.

High intensity adrenal uptake (more intense than the liver) or inhomogeneous adrenal uptake on the side of the abnormal adrenal on CT is considered abnormal. Extra-adrenal sites of uptake that cannot be explained by normal physiological distribution are considered abnormal.

#### Diagnostic Accuracy

PHEO and symp-PGL exhibit a catecholaminergic phenotype on imaging. $^{123}$I-MIBG scintigraphy has a sensitivity ranging from 83 to 100% and a very

high specificity (98–100 %) in detecting primary tumors. Its sensitivity is lower in small tumors, SDHx-related PHEO/PGL, metastatic PHEO/PGL, and head and neck PGL [42–48].

## $^{18}$F-Fluorodopa ($^{18}$F-DOPA) and Amino Acid Uptake Phenotype

### Cellular Uptake and Interference

Dihydroxyphenylalanine is the precursor of catecholamines. $^{18}$F-DOPA is taken up through neutral amino acid transporters (mainly LAT-1 and 2) and decarboxylated into $^{18}$F-Dopamine by cytosolic aromatic L-amino acid decarboxylase (AADC). There is no reported drug interaction in PHEO and PGL.

### Patient Preparation, Imaging Protocol, and Dosimetry

Patients should fast for at least 3 h prior to injection. The administration of 200 mg of carbidopa 1–2 h prior to $^{18}$F-DOPA injection has been reported to increase tumor uptake [49]. Scans are usually obtained 30–60 min after tracer injection from the base of the skull to mid-thighs (or over the whole body depending on the clinical setting). Additional early acquisition (at 10 min after tracer injection) centered over the abdomen can be performed to overcome difficulties in localizing abdominal PGL located near the hepatobiliary system due to physiological tracer elimination. The effective dose equivalent in adults range from 0.0199 to 0.0539 mSv/MBq with a higher radiation dose when combined with CT imaging.

### Normal Distribution and Abnormal Patterns

Physiological distribution includes the striatum, kidneys, ureter, bladder, pancreas, liver, gallbladder, biliary tract, and duodenum. Adrenal glands are faintly visible.

Any nonphysiological extra-adrenal focal uptake, asymmetrical adrenal uptake with concordant enlarged gland, or adrenal uptake more intense than liver with concordant enlarged gland, should be considered abnormal.

### Diagnostic Accuracy

PHEO and symp-PGL exhibit an amino acid uptake phenotype. $^{18}$F-DOPA PET/CT has a sensitivity approaching 100 % for PHEO and a very high specificity (95 %) for symp-PGL. Sensitivity is lower in SDHx-PHEO/symp-PGL.

## $^{68}$Ga DOTA-Coupled Somatostatin Agonists and Somatostatin Receptor Expression Phenotype

### Cellular Uptake and Interference

The DOTA-coupled somatostatin agonists bind to somatostatin receptors (SST) and induce rapid internalization of the ligand/receptor complex. The 3 currently available agonists have an excellent affinity for SST2: DOTATOC (Tyr3-octreotide), DOTATATE (Tyr3-octreotate), and DOTANOC (Nal3-octreotide). DOTATATE has an approximately tenfold higher affinity than DOTATOC and DOTANOC for SST2. DOTANOC binds specifically to SST5, although PHEO/PGL tumors express this subtype in only a small minority of cases.

### Patient Preparation, Imaging Protocol, and Dosimetry

$^{68}$Ga-conjugated peptides are available as "homemade radiotracers" with an extemporaneous preparation. There is no need for fasting before injection. It has been recommended to discontinue octreotide therapy (1 day for short-lived molecules and 3–4 weeks for long-acting analogs). Scans are usually obtained 45–90 min after tracer injection from the base of the skull to mid-thighs (or over the whole body depending on the clinical setting).

The effective dose ranges from 0.0042 to 0.015 μSv/MBq with higher radiation dose when CT used.

### Normal Distribution and Abnormal Patterns

Intense physiological accumulation of radioactivity is seen in the spleen (and accessory spleen if present), kidneys, ureter, bladder, adrenals, salivary glands, and pituitary. Accumulation in

the liver is usually less intense than noted in the spleen. The thyroid can be faintly visible. Additionally, variable tracer uptake is frequently found in the pancreas, particularly in the uncinate process. Prostate gland and breast glandular tissue may show diffuse, low-grade uptake.

### Diagnostic Accuracy

PHEO and symp-PGL almost always exhibit a somatostatin receptor expression phenotype. $^{68}$Ga-DOTA-SSA was found to be more sensitive to other tracers in metastatic PHEO/PGL and head and neck PGL (lesion-based detection rate approaching 100 %) [50–52]. It has been less studied in the context of nonmetastatic PHEO/symp-PGL than in other hereditary cases, such as VHL. In one study, the sensitivity of $^{68}$Ga-DOTATATE was 80 % in sporadic PHEO [53]. $^{68}$Ga-DOTA-SSA PET imaging can be falsely positive in metastatic lymph nodes due to various cancers, meningiomas, and other central nervous, inflammatory processes, and rare conditions such as fibrous dysplasia [53]. Nevertheless, this is often not a serious issue, since head and neck PGLs have a specific location and exhibit highly elevated uptake values [54].

## $^{18}$F-FDG PET and Glucose Metabolism Phenotype

### Cellular Uptake and Interference

$^{18}$F-FDG is taken up by tumor cells via glucose membrane transporters and phosphorylated by hexokinase into $^{18}$F-FDG-6P. $^{18}$F-FDG-6P does not follow further enzymatic pathways and accumulates proportionally to the glycolytic cellular rate. It is remarkable that tumors associated with TCA defect (*SDHx* mutations) exhibit an increased $^{18}$F-FDG uptake.

### Patient Preparation, Imaging Protocol, and Dosimetry

Patients must fast for at least 6 h. PHEO patients with secondary diabetes require specific instructions for glucose control. Scans are usually obtained at 60 min (45–90 min) postinjection. The effective dose equivalent is $2 \times 10^{-2}$ mSv/MBq.

### Normal Distribution and Abnormal Patterns

Physiological distribution includes brain cortex, salivary glands, lympatic tissue of the Waldeyer's ring, muscles, brown fat, myocardium, liver, kidneys and bladder, gastrointestinal tract, testis, uterus, and ovaries (before menopause). Physiologic $^{18}$F-FDG uptake in brown adipose tissue (BAT) occurs predominantly in norepinephrine secreting PHEO/PGL.

Any nonphysiological, extra-adrenal focal uptake or adrenal uptake more intense than the liver with concordant enlarged gland should be considered abnormal.

### Diagnostic Accuracy

PHEO and symp-PGL may exhibit a glucose metabolism phenotype. $^{18}$F-FDG PET uptake pattern is mainly influenced by tumor location and genetic status of patients with highly elevated uptake values in SDHx-related metastatic and nonmetastatic PHEO/PGL [55–57]. $^{18}$F-FDG PET positivity is present in about 80 % of primary PHEO. Several potential diagnoses should be considered in cases of $^{18}$F-FDG-avid adrenal masses.

## Other Tracers

Other tracers such as $^{99m}$Tc-hydrazinonicotinamide-Tyr(3)-octreotide, $^{18}$F-FDA (fluorodopamine) PET, and $^{11}$C-hydroxyephedrine ($^{11}$C-HED) are currently used, although they are less common.

## Head-to-Head Comparison Between Radiopharmaceuticals

### $^{18}$F-FDOPA or $^{68}$Ga-DOTA-SSA vs. $^{123}$I-MIBG

$^{18}$F-FDOPA [44] and $^{68}$Ga-DOTA-SSA [58–60] were found to be superior to $^{123/131}$I-MIBG in metastatic/multifocal cases of PHEO/PGL.

### $^{68}$Ga-DOTA-SSA vs. $^{18}$F-FDG

$^{68}$Ga-DOTATATE was compared to $^{18}$F-FDG in a series of 17 metastatic *SDHB*-related PHEO/PGL and identified more lesions than $^{18}$F-FDG (lesion-based detection rate of 98.6 % vs. 85.8 %) [52]. $^{68}$Ga-DOTATATE was also found to be superior to $^{18}$F-FDG in sporadic metastatic cases [51] and in head and neck PGL.

### $^{68}$Ga-DOTA-SSA vs. $^{18}$F-FDOPA

The use of $^{68}$Ga-DOTA-SSA in the context of PHEO/PGLs has been less studied than gastroenteropancreatic neuroendocrine tumors. A head-to-head comparison between $^{68}$Ga-DOTA-SSA and $^{18}$F-FDOPA PET has been performed in only five studies: one retrospective study from Innsbruck Medical University ($^{68}$Ga-DOTATOC in 20 patients with unknown genetic background) [61], 3 prospective studies from the National Institutes of Health (SDHB, head and neck PGL, and sporadic metastatic disease) ($^{68}$Ga-DOTATATE in 17 and 20 patients) [50–52], and one prospective study from La Timone university hospital ($^{68}$Ga-DOTATATE in 30 patients). In these studies, $^{68}$Ga-DOTA-SSA PET/CT detected more primary head and neck PGLs as well as *SDHx*-associated PGLs than $^{18}$F-FDOPA PET/CT [53]. By contrast, in the context of sporadic PHEO, $^{18}$F-FDOPA PET/CT may detect more lesions than $^{68}$Ga-DOTATATE [53]. One of the main drawbacks of $^{68}$Ga-DOTA-SSA is the very high physiological uptake by healthy adrenal glands [62].

## Current Role of Imaging for PHEO/ PGLs

Successful PHEO/PGL management requires an interdisciplinary team approach. Precise identification of clinical context and genetic status of patients enables a personalized use of functional imaging modalities. Currently, it is recommended to adopt a tailored approach using a diagnostic algorithm based on tumor location, biochemical phenotype, and any known genetic background (Table 7.1) [41, 63]. However, it should be underlined that selection of the appropriate imaging pathway using algorithms is, itself, somewhat challenging, because it requires information that is not always readily available at the time of investigating a suspected PHEO/PGL.

## Diagnosis of PHEO/Symp-PGL

### Adrenal Mass

The diagnosis of PHEO relies on the identification of excessive secretion of metanephrines. Functional imaging should be used in a small minority of cases such as those with suspicion of nonfunctioning PHEO on CT/MRI, mild elevation of metanephrines in the presence of an adrenal mass, acute cardiovascular complication in the critical care setting, hemorrhagic adrenal masses, and elevated metanephrines in renal insufficiency. Catecholamines can also be detected in vivo by proton single-voxel Magnetic Resonance Spectroscopy ($^{1}$H-MRS). PET imaging using $^{18}$F-FDOPA PET or $^{68}$Ga-DOTA-SSA is highly sensitive.

### Retroperitoneal Extra-adrenal Nonrenal Mass

In the presence of a retroperitoneal extra-adrenal nonrenal mass, it is important to differentiate a PGL from other tumors or lymph node involvement, including metastases. A biopsy is not always contributory or even recommended since it can carry a high risk of hypertensive crisis and tachyarrhythmia and therefore, should only be done if PHEO/PGL is ruled out in any patient presenting with signs and symptoms of catecholamine excess. Specific functional imaging studies, which are not usually performed before biochemical results are available, are very helpful in distinguishing PGLs from other tumors. $^{68}$Ga-DOTA-SSA is the first-line imaging since most patients are expected to have *SDHx* mutations.

## Diagnosis of Malignancy

Presently, there are no reliable cytological, histological, immunohistochemical, molecular, or imaging criteria for determining malignancy [64].

**Table 7.1** Stepwise molecular imaging approaches for pheochromocytoma/paraganglioma (PGL)

| Localization | Gene | First line | Second line |
|---|---|---|---|
| PHEO | *MEN2 (RET), SDHx, VHL, NF1, TMEM127, MAX* | $^{18}$F-FDOPA | $^{68}$Ga-DOTATATE |
| Symp-PGL | *VHL, SDHx, Carney triad, HIF2A, PHD1/2* | $^{68}$Ga-DOTATATE | $^{18}$F-FDOPA |
| Parasymp-PGL (head and neck) | *SDHx, SDHAF2* | $^{68}$Ga-DOTATATE | $^{18}$F-FDOPA |
| Metastatic PPGL | *SDHx (B > D), FH* | $^{68}$Ga-DOTATATE | $^{18}$F-FDG in SDHx<br>$^{18}$F-FDOPA in sporadic |

*PHEO* pheochromocytoma, *Symp PGL* sympathetic-associated paragangliomas, *Parasymp-PGL* parasympathetic-associated paragangliomas

The diagnosis of malignancy remains strictly based on the finding of metastases where chromaffin cells are not usually present, such as the lymph nodes, lung, bone, or liver.

Anatomical imaging appears sufficient for localizing PHEO. Functional imaging is probably not necessary in the preoperative workup of patients meeting the following criteria: >40 years, no family history, small (<3.0 cm) PHEO secreting predominantly metanephrine, and negative genetic testing. Functional imaging is strongly recommended for excluding metastatic disease in large adrenal tumors (>6.0 cm) and in SDHB patients. It is widely accepted that tumors with an underlying *SDHB* mutation are associated with a higher risk of aggressive behavior, development of metastatic disease, and ultimately, death. In these patients, there is a clear advantage of using $^{68}$Ga-DOTA-SSA over $^{123}$I-MIBG SPECT and even $^{18}$F-FDG in the presence of *SDHB* mutation.

## Staging

### Inherited and Symp-PGL

Beyond malignancy risk, inherited (especially *SDHx* and *VHL*) or symp-PGL raise the problem of multifocality. Based on recent published data, it is anticipated that $^{68}$Ga-DOTA-SSA will rapidly get a leading position in this setting. In absence of available $^{68}$Ga-DOTA-SSA, $^{18}$F-FDG should be preferred to $^{18}$F-FDOPA in *SDHx* patients (Fig. 7.4) whereas $^{18}$F-FDOPA appears to be an excellent first-line imaging tool in other genotypes and sporadic cases (Fig. 7.5).

### Metastatic Disease

Proper staging and early detection of metastatic disease is a key point for choosing the necessary treatment plan, follow-up, and outcome for these patients. CT, whole-body MRI, and PET imaging provide the most useful complementary information. The presence of *SDHx* mutations markedly influences sensitivity of $^{18}$F-FDG and $^{18}$F-FDOPA PET/CT, whereas $^{68}$Ga-DOTA-SSA seem to have an excellent sensitivity regardless of genetic background (Table 7.2). To date, $^{18}$F-FDOPA PET or $^{68}$Ga-DOTA-SSA may be the imaging modality of choice in the absence of a *SDHB* mutation, or when genetic status is unknown. By contrast, $^{68}$Ga-DOTA-SSA or, if not available, $^{18}$F-FDG PET, should be considered as the imaging modalities of reference for *SDHx*-related cases (Fig. 7.6).

## Image-Based Treatment of PHEOs/ PGLs

### Adrenal Sparing Surgery

Subtotal (cortical-sparing) adrenalectomy is a valid option in *MEN2, NF1,* or *VHL*. In cases with bilateral PHEO, this strategy offers the advantage of potentially avoiding steroid supplementation. Therefore, it is crucial to perform regular imaging follow-up of known PHEOs in addition to biochemical testing for determining the optimal time to schedule cortical-sparing surgery. CT is preferable over MRI due to its excellent resolution, which provides detailed anatomic locations of tumor extension within the adrenal gland and, for *MEN2* patients, the number of tumors within the

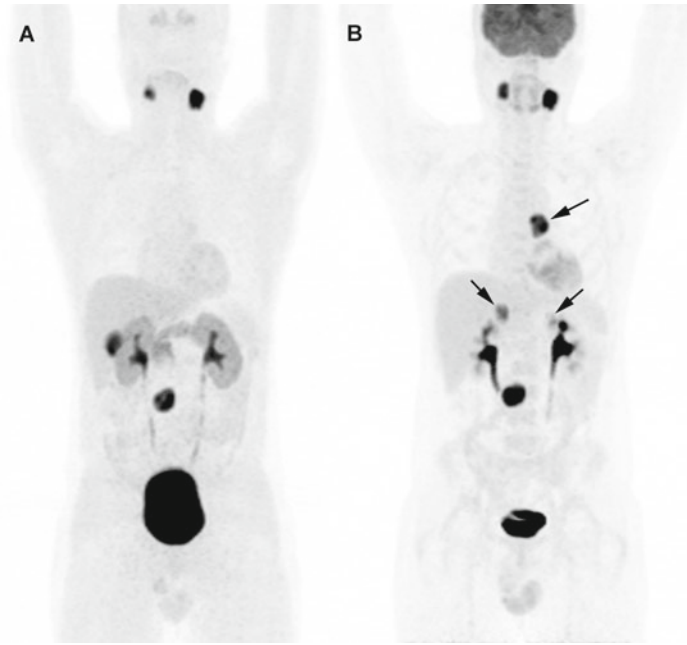


**Fig. 7.4** $^{18}$F-FDOPA (**a**) compared to $^{18}$F-FDG (**b**) in a case with multifocal SDHx-related pheochromocytoma/paraganglioma. The latter is clearly superior. Arrows indicate missed lesions on $^{18}$F-FDOPA PET/CT

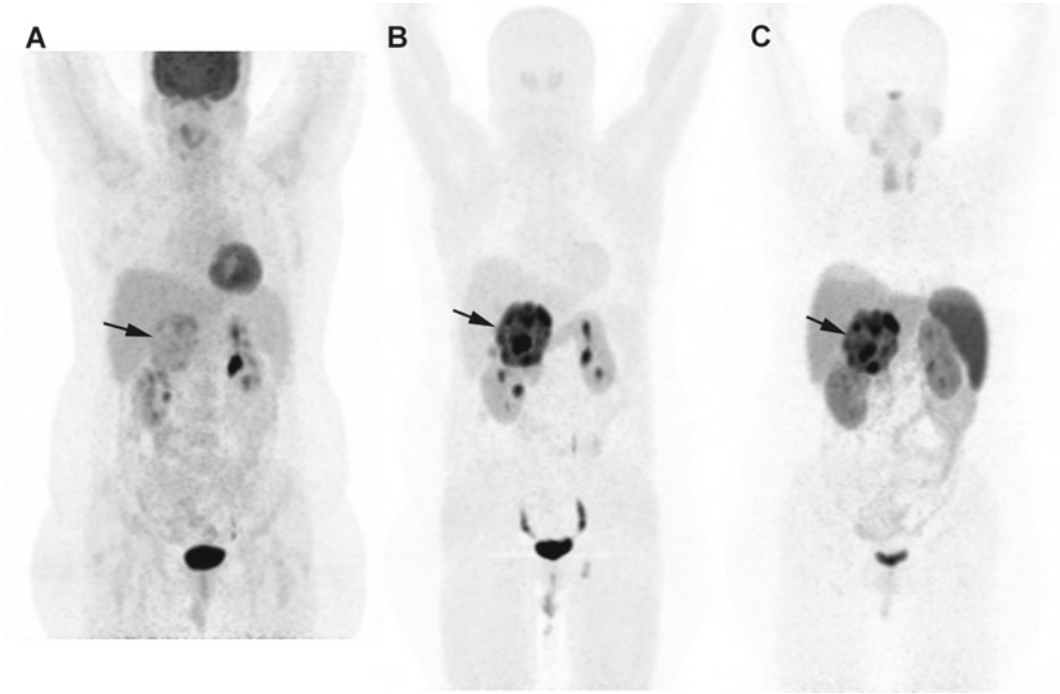


**Fig. 7.5** Head-to-head comparison of $^{18}$F-FDG (**a**), $^{18}$F-FDOPA (**b**), and $^{68}$Ga-DOTATATE (**c**) in patients with sporadic pheochromocytoma. See the low FDG tumor uptake compared to other radiopharmaceuticals

**Table 7.2** Number of identified lesions and detection rate in $^{68}$Ga-DOTATATE, $^{18}$F-FDG, $^{18}$F-FDOPA, $^{18}$F-FDA-PET/CT, and CT/MRI in metastatic *SDHB* mutation related pheochromocytoma/paraganglioma (PHEO/PGL)

| | 68Ga-DOTATATE | 18 F-FDG | 18 F-FDOPA | 18F-FDA | CT/MRI |
|---|---|---|---|---|---|
| All compartments | 294/298<br>98.7 % | 257/298<br>86.2 % | 175/285<br>61.4 % | 148/285<br>51.9 % | 254/298<br>85.2 % |
| Mediastinum | 65/65<br>100 % | 57/65<br>87.7 % | 39/65<br>60.0 % | 39/65<br>60.0 % | 55/65<br>84.6 % |
| Lungs | 62/63<br>98.4 % | 45/63<br>71.4 % | 45/63<br>71.4 % | 18/63<br>28.6 % | 62/63<br>98.4 % |
| Abdomen | 49/49<br>100 % | 46/49<br>93.9 % | 31/43<br>72.1 % | 19/43<br>44.2 % | 38/49<br>77.6 % |
| Liver | 5/5<br>100 % | 3/5<br>60.0 % | 4/5<br>80.0 % | 0/5<br>0.0 % | 5/5<br>100 % |
| Bone | 96/99<br>97.0 % | 92/99<br>92.9 % | 41/94<br>43.6 % | 57/94<br>60.6 % | 83/99<br>83.8 % |

*CT* computed tomography, *MRI* magnetic resonance imaging

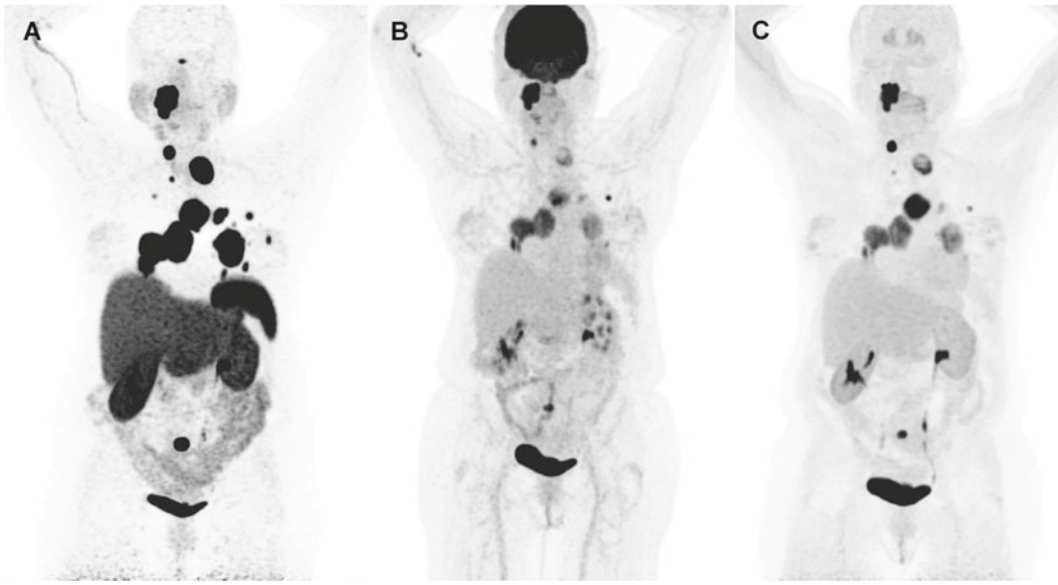


**Fig. 7.6** Superiority of $^{68}$Ga-DOTATATE to other molecular imaging modalities in *SDHB*-related metastatic pheochromocytoma/paraganglioma (PPGL). Metastatic PPGL with (**a**) $^{68}$Ga-DOTATATE, (**b**) $^{18}$F-FDG, (**c**) $^{18}$F-FDOPA

adrenal medulla. On the other hand, the advantage of using MRI over CT is the lack of exposure to ionizing radiation, which is an important factor in hereditary cases undergoing continuous follow-up. In selected cases, functional imaging may be used in addition to anatomic imaging. There is a clear advantage of $^{18}$F-FDOPA PET over MIBG and other specific PET tracers due to the lack of significant uptake in normal adrenal glands [65]. $^{18}$F-FDOPA PET may also identify metastases from medullary thyroid cancer with persistent hypercalcitoninemia.

## Theranostics

$^{123}$I-MIBG scintigraphy is used as a companion imaging agent to assist in radionuclide therapy selection. A special advantage of labeled SSAs is that, unlike $^{18}$F-FDOPA, they can be used in the radioactive treatment of these tumors (as theranostic agents). To date, peptide receptor radionuclide

therapy (PRRT) using $^{90}$Y/$^{177}$Lu-labeled somatostatin agonists has been evaluated in a limited number of PHEO/PGL cases [66–68]. On average, response rates (mainly partial responses) have been 30–60%. Disease stabilization is frequent, but more difficult to interpret since these tumors often exhibit a slow growing pattern. Larger studies including various hereditary and nonhereditary PHEO/PGLs are needed in order to conclude which PHEO/PGLs can be best treated using this therapy, and whether PRRT should be used together or as a "replacement" to other treatment modalities. Recent reports have shown that cellular internalization might shorten the residual time of $^{177}$Lu within tumor cells compared to radiolabeled SST antagonists. SST antagonists also have higher affinities for SST receptors than agonists, and lower internalization rates, resulting in a longer retention time on cell membrane. According to these observations, somatostatin antagonists might be considered as an alternative to agonists for PRRT sometime in the future.

**Acknowledgements** Aoife Kilcoyne would like to acknowledge the support of the Mac Erlaine Research Scholarship from the Academic Radiology Research Trust, St. Vincent's Radiology Group, Dublin, Ireland.

*Funding*

This research did not receive a specific grant from any funding agency in the public, commercial, or not-for-profit sector.

## References

1. Le Douarin N, Kalcheim C. The neural crest. 2nd ed. Cambridge, UK: Cambridge University Press; 1999.
2. Unsicker K, Huber K, Schober A, Kalcheim C. Resolved and open issues in chromaffin cell development. Mech Dev. 2013;130(6–8):324–9.
3. Schober A, Parlato R, Huber K, Kinscherf R, Hartleben B, Huber TB, et al. Cell loss and autophagy in the extra-adrenal chromaffin organ of Zuckerkandl are regulated by glucocorticoid signalling. J Neuroendocrinol. 2013;25(1):34–47.
4. Pena CS, Boland GW, Hahn PF, Lee MJ, Mueller PR. Characterization of indeterminate (lipid-poor) adrenal masses: use of washout characteristics at contrast-enhanced CT. Radiology. 2000;217(3):798–802.
5. Bessell-Browne R, O'Malley ME. CT of pheochromocytoma and paraganglioma: risk of adverse events with i.v. administration of nonionic contrast material. Am J Roentgenol. 2007;188(4):970–4.
6. Baid SK, Lai EW, Wesley RA, Ling A, Timmers HJ, Adams KT, et al. Brief communication: radiographic contrast infusion and catecholamine release in patients with pheochromocytoma. Ann Intern Med. 2009;150(1):27–32.
7. Kawashima A, Sandler CM, Fishman EK, Charnsangavej C, Yasumori K, Honda H, et al. Spectrum of CT findings in nonmalignant disease of the adrenal gland. Radiographics. 1998;18(2):393–412.
8. Elsayes KM, Mukundan G, Narra VR, Lewis Jr JS, Shirkhoda A, Farooki A, et al. Adrenal masses: mr imaging features with pathologic correlation. Radiographics. 2004;24 Suppl 1:S73–86.
9. Park BK, Kim CK, Kwon GY, Kim JH. Re-evaluation of pheochromocytomas on delayed contrast-enhanced CT: washout enhancement and other imaging features. Eur Radiol. 2007;17(11):2804–9.
10. Blake MA, Krishnamoorthy SK, Boland GW, Sweeney AT, Pitman MB, Harisinghani M, et al. Low-density pheochromocytoma on CT: a mimicker of adrenal adenoma. Am J Roentgenol. 2003;181(6):1663–8.
11. Brown H, Goldberg PA, Selter JG, Cabin HS, Marieb NJ, Udelsman R, et al. Hemorrhagic pheochromocytoma associated with systemic corticosteroid therapy and presenting as myocardial infarction with severe hypertension. J Clin Endocrinol Metab. 2005;90(1):563–9.
12. Leung K, Stamm M, Raja A, Low G. Pheochromocytoma: the range of appearances on ultrasound, CT, MRI, and functional imaging. Am J Roentgenol. 2013;200(2):370–8.
13. Blake MA, Kalra MK, Maher MM, Sahani DV, Sweeney AT, Mueller PR, et al. Pheochromocytoma: an imaging chameleon. Radiographics. 2004;24 Suppl 1:S87–99.
14. Northcutt BG, Trakhtenbroit MA, Gomez EN, Fishman EK, Johnson PT. Adrenal adenoma and pheochromocytoma: comparison of multidetector ct venous enhancement levels and washout characteristics. J Comput Assist Tomogr. 2016;40(2):194–200.
15. Caoili EM, Korobkin M, Francis IR, Cohan RH, Platt JF, Dunnick NR, et al. Adrenal masses: characterization with combined unenhanced and delayed enhanced CT. Radiology. 2002;222(3):629–33.
16. Szolar DH, Kammerhuber FH. Adrenal adenomas and nonadenomas: assessment of washout at delayed contrast-enhanced CT. Radiology. 1998;207(2):369–75.
17. Patel J, Davenport MS, Cohan RH, Caoili EM. Can established CT attenuation and washout criteria for adrenal adenoma accurately exclude pheochromocytoma? Am J Roentgenol. 2013;201(1):122–7.
18. Alderazi Y, Yeh MW, Robinson BG, Benn DE, Sywak MS, Learoyd DL, et al. Phaeochromocytoma: current concepts. Med J Aust. 2005;183(4):201–4.
19. Neumann HP, Berger DP, Sigmund G, Blum U, Schmidt D, Parmer RJ, et al. Pheochromocytomas, multiple endocrine neoplasia type 2, and von Hippel-Lindau disease. N Engl J Med. 1993;329(21):1531–8.
20. Quint LE, Glazer GM, Francis IR, Shapiro B, Chenevert TL. Pheochromocytoma and paraganglioma:

comparison of MR imaging with CT and I-131 MIBG scintigraphy. Radiology. 1987;165(1):89–93.
21. Velchik MG, Alavi A, Kressel HY, Engelman K. Localization of pheochromocytoma: MIBG [correction of MIGB], CT, and MRI correlation. J Nucl Med. 1989;30(3):328–36.
22. Welch TJ, Sheedy 2nd PF, van Heerden JA, Sheps SG, Hattery RR, Stephens DH. Pheochromocytoma: value of computed tomography. Radiology. 1983;148(2):501–3.
23. Jalil ND, Pattou FN, Combemale F, Chapuis Y, Henry JF, Peix JL, et al. Effectiveness and limits of preoperative imaging studies for the localisation of pheochromocytomas and paragangliomas: a review of 282 cases. French Association of Surgery (AFC), and The French Association of Endocrine Surgeons (AFCE). Eur J Surg. 1998;164(1):23–8.
24. Sahdev A, Sohaib A, Monson JP, Grossman AB, Chew SL, Reznek RH. CT and MR imaging of unusual locations of extra-adrenal paragangliomas (pheochromocytomas). Eur Radiol. 2005;15(1):85–92.
25. Ilias I, Pacak K. Current approaches and recommended algorithm for the diagnostic localization of pheochromocytoma. J Clin Endocrinol Metab. 2004;89(2):479–91.
26. Blake MA, Cronin CG, Boland GW. Adrenal imaging. Am J Roentgenol. 2010;194(6):1450–60.
27. Jacques AE, Sahdev A, Sandrasagara M, Goldstein R, Berney D, Rockall AG, et al. Adrenal phaeochromocytoma: correlation of MRI appearances with histology and function. Eur Radiol. 2008;18(12):2885–92.
28. Varghese JC, Hahn PF, Papanicolaou N, Mayo-Smith WW, Gaa JA, Lee MJ. MR differentiation of phaeochromocytoma from other adrenal lesions based on qualitative analysis of T2 relaxation times. Clin Radiol. 1997;52(8):603–6.
29. Raja A, Leung K, Stamm M, Girgis S, Low G. Multimodality imaging findings of pheochromocytoma with associated clinical and biochemical features in 53 patients with histologically confirmed tumors. Am J Roentgenol. 2013;201(4):825–33.
30. Mayo-Smith WW, Boland GW, Noto RB, Lee MJ. State-of-the-art adrenal imaging. Radiographics. 2001;21(4):995–1012.
31. Elsayes KM, Narra VR, Leyendecker JR, Francis IR, Lewis Jr JS, Brown JJ. MRI of adrenal and extraadrenal pheochromocytoma. Am J Roentgenol. 2005;184(3):860–7.
32. Mitchell DG, Crovello M, Matteucci T, Petersen RO, Miettinen MM. Benign adrenocortical masses: diagnosis with chemical shift MR imaging. Radiology. 1992;185(2):345–51.
33. Tsushima Y, Takahashi-Taketomi A, Endo K. Diagnostic utility of diffusion-weighted MR imaging and apparent diffusion coefficient value for the diagnosis of adrenal tumors. J Magn Reson Imaging. 2009;29(1):112–7.
34. Kim S, Salibi N, Hardie AD, Xu J, Lim RP, Lee VS, et al. Characterization of adrenal pheochromocytoma using respiratory-triggered proton MR spectroscopy: initial experience. Am J Roentgenol. 2009;192(2):450–4.
35. Maurea S, Cuocolo A, Reynolds JC, Neumann RD, Salvatore M. Diagnostic imaging in patients with paragangliomas. Computed tomography, magnetic resonance and MIBG scintigraphy comparison. Q J Nucl Med. 1996;40(4):365–71.
36. Ilias I, Alesci S, Pacak K. Current views on imaging of adrenal tumors. Horm Metab Res. 2004;36(6):430–5.
37. McGahan JP. Adrenal gland: MR imaging. Radiology. 1988;166(1 Pt 1):284–5.
38. Mayo-Smith WW, Lee MJ, McNicholas MM, Hahn PF, Boland GW, Saini S. Characterization of adrenal masses (<5 cm) by use of chemical shift MR imaging: observer performance versus quantitative measures. Am J Roentgenol. 1995;165(1):91–5.
39. Thompson LD. Pheochromocytoma of the Adrenal gland Scaled Score (PASS) to separate benign from malignant neoplasms: a clinicopathologic and immunophenotypic study of 100 cases. Am J Surg Pathol. 2002;26(5):551–66.
40. Takano A, Oriuchi N, Tsushima Y, Taketomi-Takahashi A, Nakajima T, Arisaka Y, et al. Detection of metastatic lesions from malignant pheochromocytoma and paraganglioma with diffusion-weighted magnetic resonance imaging: comparison with 18F-FDG positron emission tomography and 123I-MIBG scintigraphy. Ann Nucl Med. 2008;22(5):395–401.
41. Taïeb D, Timmers HJ, Hindie E, Guillet BA, Neumann HP, Walz MK, et al. EANM 2012 guidelines for radionuclide imaging of phaeochromocytoma and paraganglioma. Eur J Nucl Med Mol Imaging. 2012;39(12):1977–95.
42. Ilias I, Chen CC, Carrasquillo JA, Whatley M, Ling A, Lazurova I, et al. Comparison of 6-18F-fluorodopamine PET with 123I-metaiodobenzylguanidine and 111in-pentetreotide scintigraphy in localization of nonmetastatic and metastatic pheochromocytoma. J Nucl Med. 2008;49(10):1613–9.
43. Timmers HJ, Eisenhofer G, Carrasquillo JA, Chen CC, Whatley M, Ling A, et al. Use of 6-[18 F]-fluorodopamine positron emission tomography (PET) as first-line investigation for the diagnosis and localization of non-metastatic and metastatic phaeochromocytoma (PHEO). Clin Endocrinol (Oxf). 2009;71(1):11–7.
44. Timmers HJ, Chen CC, Carrasquillo JA, Whatley M, Ling A, Havekes B, et al. Comparison of 18F-fluoro-L-DOPA, 18F-fluoro-deoxyglucose, and 18F-fluorodopamine PET and 123I-MIBG scintigraphy in the localization of pheochromocytoma and paraganglioma. J Clin Endocrinol Metab. 2009;94(12):4757–67.
45. Fiebrich HB, Brouwers AH, Kerstens MN, Pijl ME, Kema IP, de Jong JR, et al. 6-[F-18]Fluoro-L-dihydroxyphenylalanine positron emission tomography is superior to conventional imaging with (123) I-metaiodobenzylguanidine scintigraphy, computer tomography, and magnetic resonance imaging

in localizing tumors causing catecholamine excess. J Clin Endocrinol Metab. 2009;94(10):3922–30.
46. Kaji P, Carrasquillo JA, Linehan WM, Chen CC, Eisenhofer G, Pinto PA, et al. The role of 6-[18F]fluorodopamine positron emission tomography in the localization of adrenal pheochromocytoma associated with von Hippel-Lindau syndrome. Eur J Endocrinol. 2007;156(4):483–7.
47. Hoegerle S, Nitzsche E, Altehoefer C, Ghanem N, Manz T, Brink I, et al. Pheochromocytomas: detection with 18 F DOPA whole body PET—initial results. Radiology. 2002;222(2):507–12.
48. Fonte JS, Robles JF, Chen CC, Reynolds J, Whatley M, Ling A, et al. False-negative 123I-MIBG SPECT is most commonly found in SDHB-related pheochromocytoma or paraganglioma with high frequency to develop metastatic disease. Endocr Relat Cancer. 2012;19(1):83–93.
49. Timmers HJ, Hadi M, Carrasquillo JA, Chen CC, Martiniova L, Whatley M, et al. The effects of carbidopa on uptake of 6-18F-Fluoro-L-DOPA in PET of pheochromocytoma and extraadrenal abdominal paraganglioma. J Nucl Med. 2007;48(10):1599–606.
50. Janssen I, Chen CC, Taieb D, Patronas NJ, Millo CM, Adams KT, et al. 68Ga-DOTATATE PET/CT in the localization of head and neck paragangliomas compared with other functional imaging modalities and CT/MRI. J Nucl Med. 2016;57(2):186–91.
51. Janssen I, Chen CC, Millo CM, Ling A, Taieb D, Lin FI et al. PET/CT comparing Ga-DOTATATE and other radiopharmaceuticals and in comparison with CT/MRI for the localization of sporadic metastatic pheochromocytoma and paraganglioma. Eur J Nucl Med Mol Imaging. 2016. [Epub ahead of print].
52. Janssen I, Blanchet EM, Adams K, Chen CC, Millo CM, Herscovitch P, et al. Superiority of [68Ga]-DOTATATE PET/CT to other functional imaging modalities in the localization of SDHB-associated metastatic pheochromocytoma and paraganglioma. Clin Cancer Res. 2015;21(17):3888–95.
53. Archier A, Varoquaux A, Garrigue P, Montava M, Guerin C, Gabriel S, et al. Prospective comparison of (68)Ga-DOTATATE and (18)F-FDOPA PET/CT in patients with various pheochromocytomas and paragangliomas with emphasis on sporadic cases. Eur J Nucl Med Mol Imaging. 2016;43(7):1248–57.
54. Hofman MS, Lau WF, Hicks RJ. Somatostatin receptor imaging with 68Ga DOTATATE PET/CT: clinical utility, normal patterns, pearls, and pitfalls in interpretation. Radiographics. 2015;35(2):500–16.
55. Taïeb D, Timmers HJ, Shulkin BL, Pacak K. Renaissance of (18)F-FDG positron emission tomography in the imaging of pheochromocytoma/paraganglioma. J Clin Endocrinol Metab. 2014;99(7):2337–9.
56. Timmers HJ, Chen CC, Carrasquillo JA, Whatley M, Ling A, Eisenhofer G, et al. Staging and functional characterization of pheochromocytoma and paraganglioma by 18 F-fluorodeoxyglucose (18F-FDG) positron emission tomography. J Natl Cancer Inst. 2012;104(9):700–8.
57. Timmers HJ, Kozupa A, Chen CC, Carrasquillo JA, Ling A, Eisenhofer G, et al. Superiority of fluorodeoxyglucose positron emission tomography to other functional imaging techniques in the evaluation of metastatic SDHB-associated pheochromocytoma and paraganglioma. J Clin Oncol. 2007;25(16):2262–9.
58. Sharma P, Dhull VS, Arora S, Gupta P, Kumar R, Durgapal P, et al. Diagnostic accuracy of (68)Ga-DOTANOC PET/CT imaging in pheochromocytoma. Eur J Nucl Med Mol Imaging. 2014;41(3):494–504.
59. Naswa N, Sharma P, Nazar AH, Agarwal KK, Kumar R, Ammini AC, et al. Prospective evaluation of (6)(8) Ga-DOTA-NOC PET-CT in phaeochromocytoma and paraganglioma: preliminary results from a single centre study. Eur Radiol. 2012;22(3):710–9.
60. Kroiss A, Shulkin BL, Uprimny C, Frech A, Gasser RW, Url C, et al. (68)Ga-DOTATOC PET/CT provides accurate tumour extent in patients with extraadrenal paraganglioma compared to (123)I-MIBG SPECT/CT. Eur J Nucl Med Mol Imaging. 2015;42(1):33–41.
61. Kroiss A, Putzer D, Frech A, Decristoforo C, Uprimny C, Gasser RW, et al. A retrospective comparison between (68)Ga-DOTA-TOC PET/CT and (18)F-DOPA PET/CT in patients with extra-adrenal paraganglioma. Eur J Nucl Med Mol Imaging. 2013;40(12):1800–8.
62. Kroiss A, Putzer D, Decristoforo C, Uprimny C, Warwitz B, Nilica B, et al. 68Ga-DOTA-TOC uptake in neuroendocrine tumour and healthy tissue: differentiation of physiological uptake and pathological processes in PET/CT. Eur J Nucl Med Mol Imaging. 2013;40(4):514–23.
63. Lenders JW, Duh QY, Eisenhofer G, Gimenez-Roqueplo AP, Grebe SK, Murad MH, et al. Pheochromocytoma and paraganglioma: an endocrine society clinical practice guideline. J Clin Endocrinol Metab. 2014;99(6):1915–42.
64. Gimm O, DeMicco C, Perren A, Giammarile F, Walz MK, Brunaud L. Malignant pheochromocytomas and paragangliomas: a diagnostic challenge. Langenbecks Arch Surg. 2012;397(2):155–77.
65. Luster M, Karges W, Zeich K, Pauls S, Verburg FA, Dralle H,etal.Clinicalvalueof18F-fluorodihydroxyphenylalanine positron emission tomography/computed tomography (18F-DOPA PET/CT) for detecting pheochromocytoma. Eur J Nucl Med Mol Imaging. 2010;37(3):484–93.
66. van Essen M, Krenning EP, Kooij PP, Bakker WH, Feelders RA, de Herder WW, et al. Effects of therapy with [177Lu-DOTA0, Tyr3]octreotate in patients with paraganglioma, meningioma, small cell lung carcinoma, and melanoma. J Nucl Med. 2006;47(10):1599–606.
67. Zovato S, Kumanova A, Dematte S, Sansovini M, Bodei L, Di Sarra D, et al. Peptide receptor radionuclide therapy (PRRT) with 177Lu-DOTATATE in individuals with neck or mediastinal paraganglioma (PGL). Horm Metab Res. 2012;44(5):411–4.
68. Puranik AD, Kulkarni HR, Singh A, Baum RP. Peptide receptor radionuclide therapy with Y/Lu-labelled peptides for inoperable head and neck paragangliomas (glomus tumours). Eur J Nucl Med Mol Imaging. 2015;42(8):1223–30.